Dielectric Normal Mode Relaxation of Probe Polyisoprene Chain in Semidilute Polybutadiene Solutions. 2. Dynamic Behavior

Osamu Urakawa, Keiichiro Adachi,* and Tadao Kotaka

Department of Macromolecular Science, Faculty of Science, Osaka University, Toyonaka, Osaka 560, Japan

Received November 3, 1992; Revised Manuscript Received January 14, 1993

ABSTRACT: Dynamics of a trace amount of *cis*-polyisoprene (PI) dissolved in semidilute polybutadiene (PB)/*n*-heptane (Hep) solutions as a probe was examined through dielectric *normal mode* relaxation studies and compared with the results of semidilute PI/Hep solutions. In PI/Hep solutions, the logarithm of the normal mode relaxation time τ of PI increased linearly with PI concentration C_I, and log τ values for different PI molecular weight M_I were superposed by plotting against $C_I[\eta]_I$ with $[\eta]_I$ being the intrinsic viscosity of PI in Hep. For the PI/PB/Hep ternary solutions of varying PB concentration C_B and molecular weight M_B, the data of τ reduced by τ_0 at the infinite dilution were plotted against the reduced concentrations $C_B[\eta]_B$ and $C_B[\eta]_I$. We found that data of τ/τ_0 were expressed by a universal function of such two parameters $C_B[\eta]_B$ and $C_B[\eta]_I$. The $\log(\tau/\tau_0)$ vs $\log(C_B[\eta]_I)$ curves under constant $C_B[\eta]_B$ exhibited a sigmoidal shape, becoming independent of $C_B[\eta]_I$ at high $C_B[\eta]_I$. The $\log(\tau/\tau_0)$ vs $\log(C_B[\eta]_B)$ curves under constant $C_B[\eta]_I$ were also cast into a universal curve of a sigmoidal shape. These curves were thus divided into three regimes in which the dynamics of the probe PI chains can be explained by a nondraining Zimm model, by a free-draining Rouse model, and by a reptation model reflecting entanglements among the PI and matrix PB chains.

Introduction

In part 1 of this series,[1] we reported conformational properties of *cis*-polyisoprene (PI) chains dissolved in semidilute solutions of polybutadiene (PB) in *n*-heptane (Hep) via the comparison of the mean square end-to-end distance $\langle r^2 \rangle$ of the PI chains determined from their dielectric relaxation strengths in the PI/PB/Hep ternary and PI/Hep binary solutions. In the ternary system, the excluded volume effect was shielded with increasing concentration C_B of PB. The C_B dependence of $\langle r^2 \rangle$ was thus approximately expressed by a universal function of C_B/C_B^*, where C_B^* is the overlapping concentration of the probe PI chains in the same systems.

Dynamics of polymer chains in semidilute and concentrated solutions has been extensively studied by various experimental techniques (e.g., Ferry[2] and Doi-Edwards[3]). Among varieties of experimental methods, dielectric normal mode spectroscopy provides a unique technique for studying the fluctuation of an end-to-end vector when sample polymers have dipole moments aligned parallel to the chain contour.[4,5] Stockmayer[4] classified such polymers as type A, and we found that PI is one of the type A polymers.[6-8]

Although binary solutions have been studied extensively, study on polymer chain dynamics in ternary systems is rare. Recently Baysal and Stockmayer studied the dielectric normal mode relaxation in the poly(ε-caprolactone)/poly(4-chlorostyrene)/dioxane ternary system.[9] So far, tracer diffusion in ternary systems has been extensively studied by several authors.[10-12] Wheeler et al.[10] determined the tracer diffusion coefficient D_{tr} by dynamic light scattering for a trace amount of polystyrene (PS) in solutions of poly(vinyl methyl ether) (PVME)/*o*-fluorotoluene. They reported that D_{tr} of the tracer PS was proportional to $M^{-\beta}$ at all PVME concentrations C_{PVME} studied and the exponent β gradually increased with increasing C_{PVME} from 0.55 in pure solvent to 1.89 at the highest PVME concentration of 0.1 g cm^{-3}, where PVME chains were presumably entangled. The diffusion of tracer PS chain is considered to be changed from Zimm type (Stokes-Einstein diffusion) (β = 0.55) to the reptation mechanism (β = 1.82), and the crossover concentration region is very broad. Such a change of the polymer dynamics may be mainly originated from the topological and hydrodynamic interactions.

Nemoto et al.[11] investigated the sedimentation coefficient S of a tracer poly(methyl methacrylate) (PMMA) in semidilute solutions of PS/thiophenol. They attempted to separate the topological and hydrodynamic interactions by investigating two extreme cases. One was the case of $M_{PMMA} \gg M_{PS}$, where PS chains are not entangled and hence the topological interaction is negligible. The other was that of $M_{PMMA} \ll M_{PS}$, where the topological interaction is dominant. They concluded that the hydrodynamic interaction becomes less dominant with decreasing M_{PMMA}/M_{PS} ratio, but even at high C_{PS}, where PS chains well overlapped, this interaction still exists when $M_{PMMA}/M_{PS} \gg 1$. However, in the case of $M_{PMMA} < M_{PS}$, the S for the tracer PMMA becomes a function of M_{PMMA}/M_e (PS), where M_e (PS) denotes the molecular weight between entanglements in the matrix PS solution. The S is now governed by the topological interaction between the matrix chains.

Numasawa et al.[12] used dynamic light scattering to investigate diffusion of the PS tracer in semidilute benzene solutions of PMMA. They showed that even when the matrix chains are entangled in the solution, the long guest chain behaves like a Zimm chain diffusing via the Stokes-Einstein mechanism and suggested that the hydrodynamic interaction becomes much more effective than the topological interaction when the guest chain is much longer than the matrix chain.

Theoretically, the diffusion coefficient corresponds to the zeroth normal mode.[3] On the other hand, the dielectric normal mode relaxation time corresponds to the first mode. So far, no studies of the first normal mode in ternary systems have been reported. In this study, we attempted to seek a universal equation based on scaling theory to describe the concentration dependence of the longest relaxation time of tracer chains in semidilute solutions of foreign polymers using tracer PI in PB/Hep solutions. For the sake of comparison, we also studied the dielectric normal mode relaxation in PI/Hep binary solutions.

0024-9297/93/2226-2042$04.00/0

Theory

We briefly review the theories of the normal mode relaxation. When chains are not entangled, the bead-spring model proposed by Rouse[13] and Zimm[14] is applied. According to the nondraining Zimm theory, the relaxation time for the pth normal mode is given by

$$\tau_p = 1.61\eta_s N^{3/2} b^3/\lambda_p k_B T \propto (\eta_s r^3) \quad (1)$$

where N is the number of beads, b is the average distance between beads, λ_p is the eigen value, η_s is the solvent viscosity, and r is the end-to-end distance. This equation holds in the Θ state. In good solvent eq 1 is approximately given by[3]

$$\tau_p \propto \eta_s N^{3\nu} b^3/(p^{3\nu} k_B T) \propto \eta_s r^3 \quad (2)$$

where ν is the excluded volume exponent equal to $^3/_5$ in a good solvent and $^1/_2$ in a Θ solvent. The free-draining Rouse model predicts

$$\tau_p = \zeta N^2 b^2/(p^2 k_B T) \quad (3)$$

where ζ is the friction constant per bead. In an entangled region τ is expressed by the tube model proposed by de Gennes[15] and Doi and Edwards[3,16]

$$\tau_p = \zeta N^3 b^4/a^2 p^2 k_B T \quad (4)$$

where a is the distance between entanglements.

In dilute polymer solutions, hydrodynamic interaction acts upon the whole chain. In semidilute solutions, such interaction is screened over the distance of screening length (correlation length) ξ but works within ξ. To take into account such interaction, the dynamic scaling theory[17,18] successfully explained the dynamics in semidilute solutions by replacing the g units of segments by a blob having a dimension ξ where $g \simeq C^{1/(1-3\nu)}$ and $\xi \simeq bg^{\nu}$. In eqs 2–4 we replace N by N/g, b by ξ, and ζ by the fraction ζ_{blob} per blob equal to $6\pi\eta_s\xi$ (Stokes–Einstein relation). Then τ reduced by the relaxation time τ_0 at infinite dilution is expressed only by a parameter C/C^*, where C^* ($\simeq N^{1-3\nu}$) is the overlapping concentration.[17] Equation 2 does not change by such replacement since the hydrodynamic interaction works within and out of the blob equally. When chains are overlapped but not still in the entangled regime, τ is given by

$$\tau \simeq \tau_0 (C/C^*)^{(2-3\nu)/(3\nu-1)} \quad (5)$$

In the entangled regime, τ is given by

$$\tau \simeq \tau_0 (C/C^*)^{(3-3\nu)/(3\nu-1)} \quad (6)$$

Since the $\tau \propto N^{3.0}$ dependence proposed by the tube theory has not been observed, eq 6 is often modified[19] by using the well-known empirical relation $\tau \propto N^{3.4}$.

$$\tau \simeq \tau_0 (C/C^*)^{(3.4-3\nu)/(3\nu-1)} \quad (7)$$

Muthukumar and Freed[20,21] described the C dependence of the relaxation time τ_p in the crossover region from dilute to semidilute regime

$$\tau_p = \tau_{p0}[1 + CAp^{-\kappa} - 2^{0.5}(CAp^{-\kappa})^{1.5} + 2(CAp^{-\kappa})^{2.0} + ...] \quad (8)$$

where τ_{p0} is the relaxation time at infinite dilution, A is the constant proportinal to $M^{(3\nu-1)}$, and κ is the constant equal to $3\nu - 1$. It is noted that A is proportional to the intrinsic viscosity $[\eta]$. At sufficiently low concentration region τ_1 is approximately written as

$$\tau_1 \simeq \tau_{10} \exp(CA) \quad (9)$$

This equation predicts that log τ_1 is proportional to CA.

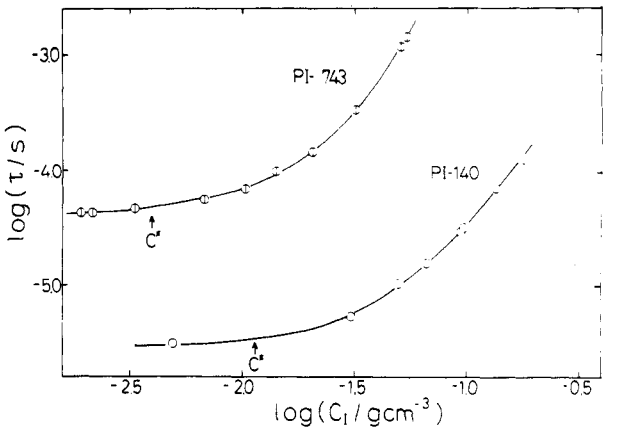

Figure 1. Concentration dependence of the normal mode relaxation time τ in n-heptane solutions of PI-743 and PI-140 at 295 K.

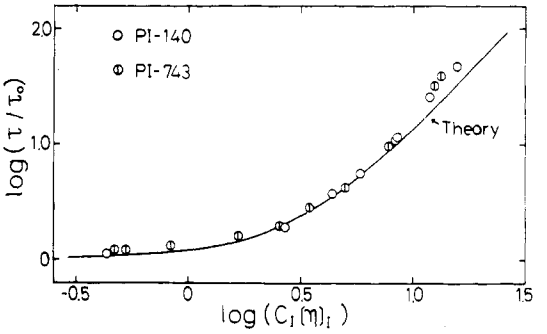

Figure 2. Double-logarithmic plot of τ/τ_0 vs $C_I[\eta]_I$ for PI-743 and PI-140 in n-heptane, where τ_0 is the relaxation time at infinite dilution. The solid line indicates the Muthukumar and Freed theory given by eq 7.

Experimental Section

All PI and PB samples were prepared in n-heptane at 20 ± 5 °C by anionic living polymerization with *sec*-butyllithium as an initiator. Their characteristics are described in part 1 of this series.[1] The samples are coded with PI and PB plus a figure representing the weight-average molecular weight in units of kilograms per mole. Methods of dielectric measurements were also described in part 1. Relative viscosity of PI solutions were measured with an Ubbelohde-type viscometer at 295 K.

Results and Discussion

1. PI/Heptane Binary Systems. 1.1. Concentration Dependence of the Relaxation Time. First we report the results for the binary PI/heptane system. The relaxation time τ_n for the normal mode process was determined by the relation $\tau_n = 1/(2\pi f_m)$, where f_m is the loss maximum frequency. If the normal mode relaxation is described by the Rouse or Doi–Edwards theory, τ_n is equal to $0.97\tau_1$, where τ_1 is the relaxation time for the first normal mode. The dependences of τ_n on concentration C_I of PI are shown in Figure 1 for solutions of PI-140 and PI-743. It is seen that τ increases strongly when C increases beyond C^*. This is due to the chain overlapping and entanglement effect.

Figure 2 shows the double-logarithmic plots of τ/τ_0 vs $C[\eta]$ ($\simeq C/C^*$). In spite of the relatively large difference of M, two curves for PI-743 and PI-140 coincide well. The theories predict that in low concentration τ_1 is given by the Zimm theory (eq 2) but in high concentration regions

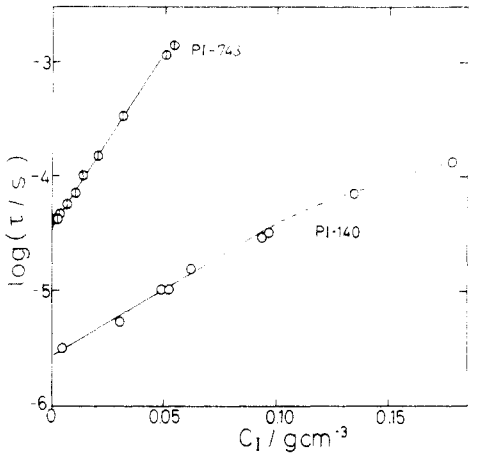

Figure 3. Logarithm of τ vs C_I for PI-743 and PI-140 solutions.

τ_1 conforms to eqs 5 and 7. However, the transition from nonentangled to entangled region is ambiguous.

Figure 3 shows the test of the Muthukumar–Freed theory,[20,21] namely and semilogarithmic plots of log τ vs C for solutions of PI-743 and PI-140. In the low-concentration region, log τ data are well represented by the straight lines and agree with eq 9. The parameter A can be determined from the slope of straight lines: for PI-743 A is 70.0 and for PI-140 A is 26.2. This value of A is equal to $0.29[\eta]$ within the 6% experimental error. The solid line in Figure 2 shows the theoretical τ_1 calculated by eq 8 with $\nu = 0.56$ and $p = 1$. We see that eq 8 successfully describes the concentration dependence of τ_1 up to $C[\eta] \simeq 8$. Recently Patel and Takahashi[22] reported the dielectric normal mode relaxation of *cis*-polyisoprene in semidilute solutions in a moderately good solvent, Isopar-G. They reported that τ_1/τ_{10} is a universal function of CA rather than of $C[\eta]$. However, if the data are cast into the Muthukumar theory, A becomes equal to $0.294[\eta]$. This agrees with our result.

Baysal and Stockmayer[9] carried out dielectric measurement on the ternary system of poly(ϵ-caprolactone) (PCL)/poly(4-chlorostyrene) (PCST)/dioxane in which PCL has the type A dipole. They expressed the concentration dependence of the τ_1 of PCL as $\tau_1 = \tau_{10}\{1 + B(C_A[\eta]_A + C_B[\eta]_B)\}$, where the subscripts A and B denote PCL and PCST, respectively. The factor B was determined to be 0.35.[9] The same analysis has been made for the τ_1 of PI in the PI/PB/Hep ternary system, which is described in detail later. We have obtained B to be 0.28, which is close to the factor for the PI/Hep binary system. We are unable to explain the difference of B between PCL and PI.

1.2. Shape of ϵ'' Curves. Figure 4 shows the comparison of the shape of ϵ'' curves reduced by the ϵ''_{max} and f_{max} for PI-743 solutions. We see that the curves become broad with increasing C_I. For the dilute solutions, the width is nearly equal to that predicted by the Rouse or Zimm theory.[13,14] For the semidilute solutions, the curves become broad in the high-frequency region with increasing C_I. As described in part 1, the log ϵ'' vs log f curve is straight in the range of 0.5 decade above the f_{max}. With increasing concentration the slope α (=dlog ϵ''/dlog f) in the high-frequency side of the loss curve decreases. This phenomenon cannot be explained on the basis of the Zimm, Rouse, or tube theory: As was pointed out frequently in our previous papers,[6] all of these theories predict that the intensity of the pth mode is proportional to $1/p^2$. It is sure that the interchain interaction makes the mode distribution change, but the detailed mechanism is not known.

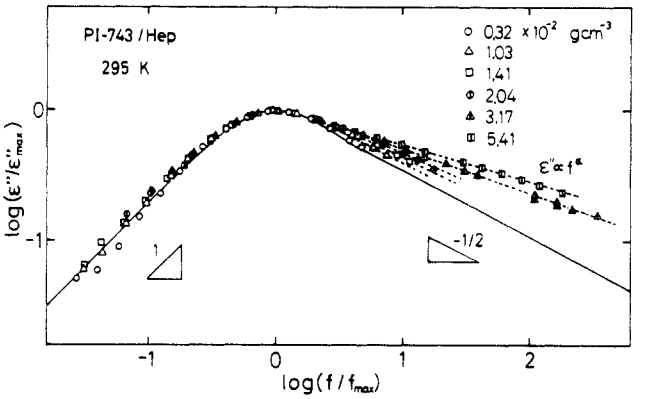

Figure 4. Double-logarithmic plot of reduced ϵ'' curves at 295 K for PI-743 solutions of various concentrations. The solid line indicates the Rouse and tube theory.

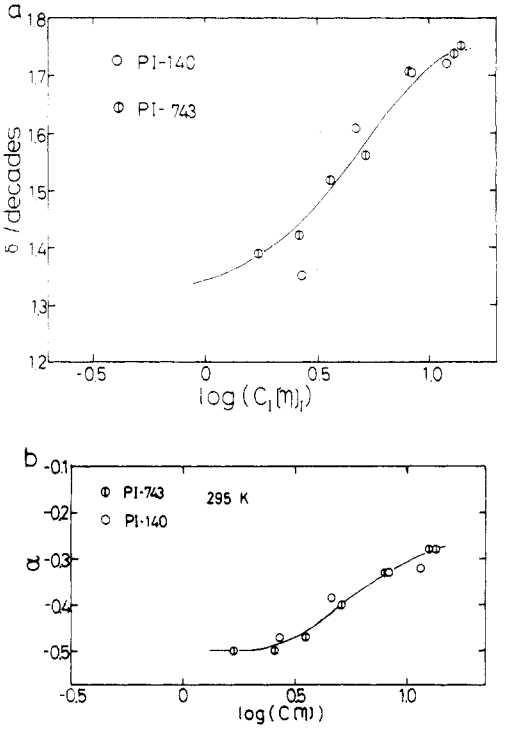

Figure 5. (a) Dependence of the half-width Δ of the ϵ'' curve on $C_I[\eta]_I$ for PI-743 and PI-140 solutions. (b) Slope α of log ϵ'' vs log f curve in the high-frequency side for PI-743 and PI-140 solutions.

Examining the ϵ'' curve carefully, we found that the half-width δ begins to increase around $C_I \simeq C_I^*$. Thus, we plotted δ and α against $C_I[\eta]_I$ in Figure 5. As is seen in this figure, the δ or α vs $C_I[\eta]_I$ plots for PI-743 and PI-140 almost coincide. This result suggests that the mode distribution can be expressed by a universal function of $C[\eta]$. The scaling theory predicts that the chain dynamics is expressed universally as a function of $C[\eta]$ as long as the frequency range is not too high compared with the inverse of the time scale for the motion in the screening length (in the blob). Thus, our experimental result is reasonable. The change in the dynamics with increasing C_I is caused by the interchain interactions, and the changing process is scaled by $C[\eta]$.

2. PI/PB/Heptane Ternary System. 2.1. C_B and M_B Dependence of τ. In this section the dynamic behavior in the PI/PB/Hep system is reported. It is noted that PI concentration C_I is regulated so that the PI chains do not overlap each other. The concentration C_B of PB was changed widely.

Figure 6 shows the C_B dependence of τ for PI-140, PI-

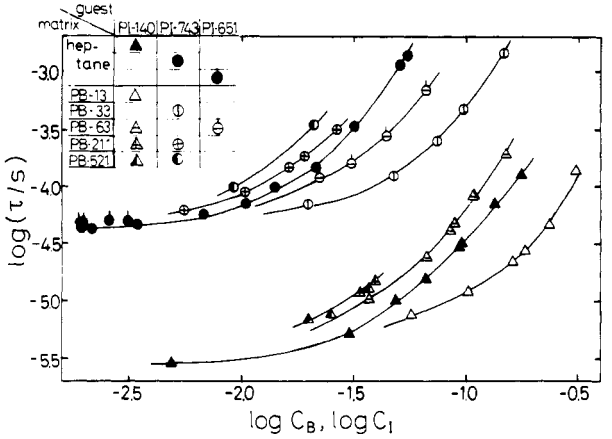

Figure 6. PB concentration C_B dependence of τ of PI in ternary solutions at 295 K. The data of binary PI/heptane systems are plotted against PI concentration C_I with solid symbols. The solid lines are a guide for the eyes.

743, and PI-651 in PB semidilute solution. The values of τ in PI/Hep binary solutions are also plotted against C_I with the solid symbols. It is seen that at fixed molecular weight M_B of PB, τ of PI increases with C_B and at fixed C_B, τ increases with M_B. Since C_I is kept less than the overlapping concentration, the increase in τ is caused by overlapping or entanglement between the PI and PB chains.

2.2. Theoretical Expression of τ by Scaling Theory. The complex C_B and M_B dependences of τ were analyzed in terms of the blob model for two extreme cases: $M_I \gg M_B$ and $M_I \ll M_B$.

2.2.1. $M_I \gg M_B$. For dilute solutions of the PI chain, the relaxation time τ_0 is predicted by eq 2

$$\tau_0 \simeq \eta_s r_0^3/k_B T \tag{10}$$

where r_0 is the end-to-end distance at infinite dilution. For the ternary solutions, this equation may be correct when C_B is smaller than C_B^*. As was demonstrated in the study of diffusion, we expect that even in the range $C_B > C_B^*$ eq 10 holds if $M_I \gg M_B$. In such case, the PB chains move much faster than the PI chain and act as solvents

$$\tau \simeq \eta_B r^3/k_B T \tag{11}$$

where η_B is the viscosity of a PB solution and r the end-to-end distance of the PI chain in the PB solution. In eqs 10 and 11, the numerical factor is considered to be the same. Thus, from these equations, we derive

$$\tau/\tau_0 = (\eta_B/\eta_s)(r/r_0)^3 \tag{12}$$

The ratio of $\langle r^2\rangle/\langle r^2\rangle_0$ has been reported in part 1 of this series[1] and approximately conformed to a universal function f of $C_B[\eta]_B$ in the case of $M_I > M_B$:

$$\langle r^2\rangle/\langle r^2\rangle_0 \simeq f(C_B[\eta]_B) \tag{13}$$

It is well-known that η_B/η_s in semidilute solutions is approximately expressed by a universal function g of $C_B[\eta]_B$[19]

$$\eta_B/\eta_s \simeq g(C_B[\eta]_B) \tag{14}$$

where g represents a function. Combining eqs 12–14, we obtain

$$\tau/\tau_0 \simeq F_1(C_B[\eta]_B) \tag{15}$$

where F_1 is a function. This equation predicts that when the PI chain behaves like a Zimm chain, τ of the single PI chain in various MW matrices of PB is expressed by a universal function of $C_B[\eta]_B$.

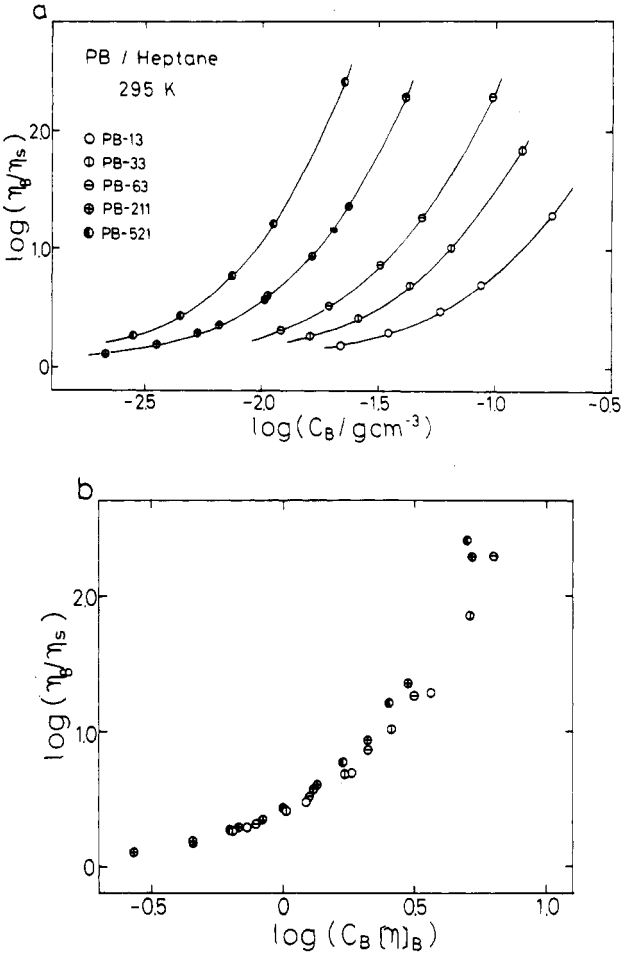

Figure 7. (a) Double-logarithmic plot of relative viscosity η_B/η_s vs PB concentration C_B at 295 K for PB/heptane solutions at 295 K. (b) Same data plotted against $C_B[\eta]_B$.

2.2.2. $M_I \ll M_B$. Next we consider the opposite case of $M_I \ll M_B$. In this case the matrix PB chain is regarded as a fixed network and the PI chains move under constraints of the network.[15-18] τ of PI may be determined by the tube diameter a being equal to the distance between entanglements of PB chain and friction coefficient ζ_{blob} per blob. According to de Gennes[18] and recent experimental data,[19] a is proportional to the blob size ξ_B of PB matrix solution and ζ_{blob} is also proportional to the blob size as is given by the Stokes law for a nondraining sphere. We assume that the size of the blob of PI is equal to that of PB. Then τ is given by

$$\tau \simeq \tau_{blob} f'(N_I/g_B) \tag{16}$$

where f' represents a function, τ_{blob} ($\propto \xi_B^2\zeta_{blob}$) is the relaxation time for the single free blob, N_I is the degree of polymerization of the PI, and g_B is the number of monomeric units of PB in the single blob. τ_0 in eq 10 is scaled by the blob and is rewritten as

$$\tau_0 \simeq \tau_{blob}(N_I/g_B)^{3\nu} \tag{17}$$

From eqs 16 and 17, τ is written in the form

$$\tau \simeq \tau_0 F_2(C_B[\eta]_I) \tag{18}$$

where F_2 is the function.

2.3. Analysis of Experimental τ. To test eqs 12, 14, and 18, we measured the relative viscosity η_B/η_s and plotted it in Figure 7a. These data are also plotted against $C_B[\eta]_B$ in Figure 7b. We see that η_B/η_s is approximately expressed by a universal function in accordance with the result reported by Takahashi et al.[19] and others.[23-25] In Figure

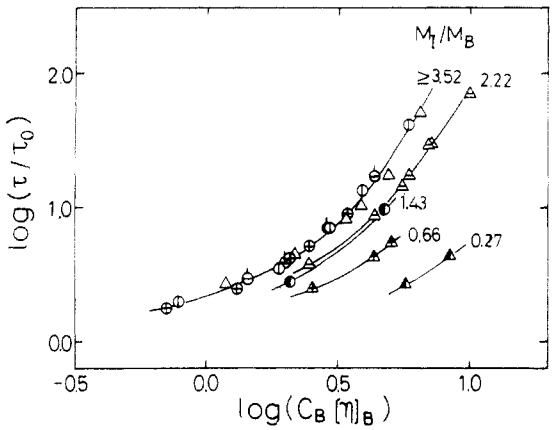

Figure 8. Double-logarithmic plot of τ/τ_0 vs $C_B[\eta]_B$. The ratio of M_I/M_B is indicated in the curve. The symbols are the same as in Figure 6.

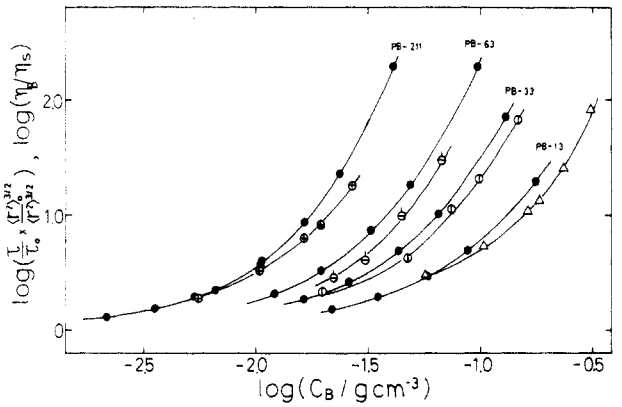

Figure 9. Comparison of the viscosity of PB matrix solutions with the relaxation times of PI reduced by the chain dimension. The symbols are the same as in Figure 6.

7b we see that the curves slightly shift downward with decreasing M_B. We may ignore this effect here.

Figure 8 shows the test of eq 15, namely the double-logarithmic plot of τ/τ_0 vs $C_B[\eta]_B$. As is seen in the figure, the data points in the range $M_I/M_B > 3.52$ conform to a universal curve. Thus, we conclude that there is a regime in which eq 15 holds.

Obviously this dos not necessarily mean that the PI chain is Zimm-like. Thus, we checked eq 12 directly. Figure 9 shows the concentration dependences of $(\tau/\tau_0)(r_0/r)^3$ and η_B/η_s. If eq 12 is valid, the $(\tau/\tau_0)(r_0/r)^3$ and η_B/η_s curves should coincide. As is seen in the figure, the viscosity is slightly larger than the relaxation time for all systems. The discrepancy may be attributed to the following two origins: (1) the PI chains are not Zimm-like depending on the conditions and (2) the macroscopic viscosity differs from the effective viscosity for the PI chain.

Figure 10 shows the test of eq 18, namely the double-logarithmic plot of τ/τ_0 vs $C_B[\eta]_I$. We see that the data points for $M_I/M_B < 1.43$ conform to a universal curve, indicating that there exists a regime where eq 18 holds.

Nemoto et al.[11] showed that the sedimentation coefficient S of PMMA in high MW PS solutions was expressed as

$$S/S(0.1M_e(\mathrm{PS})) \simeq H(M/M_e(\mathrm{PS})) \qquad (19)$$

where $S(0.1M_e(\mathrm{PS}))$ indicates the sedimentation coefficient of PMMA with MW equal to $0.1M_e$(PS) and H is a topological function. We see that this equation has the same functional form as eq 16 because $S(0.1M_e(\mathrm{PS}))$ and $M/M_e(\mathrm{PS})$ correspond to τ_{blob} and N_I/g_B, respectively, by considering the proportionality $M_e \propto g$.[22]

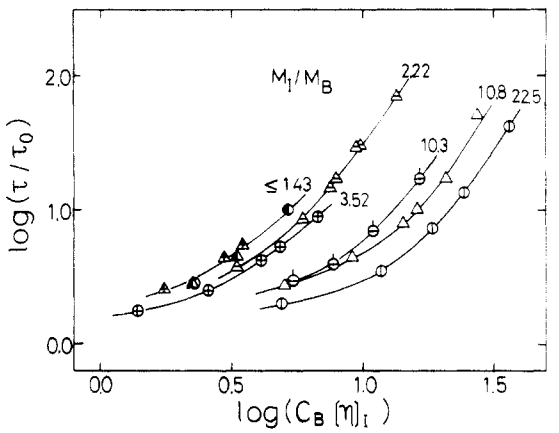

Figure 10. Double-logarithmic plot of τ/τ_0 vs $C_B[\eta]_I$. The symbols are the same as in Figure 6.

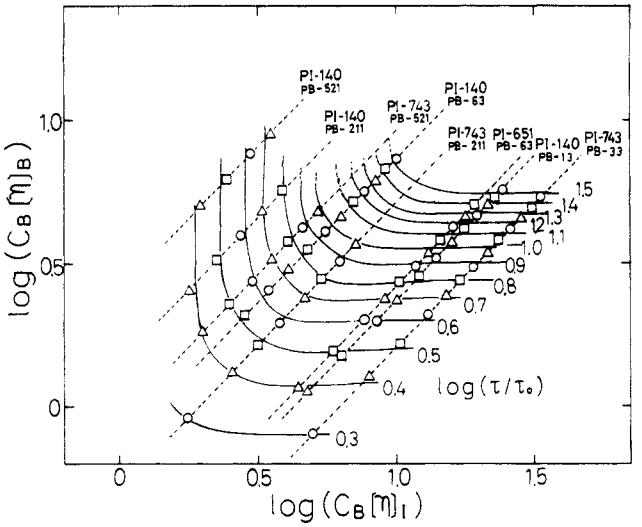

Figure 11. Iso-τ/τ_0 lines on the plane of $C_B[\eta]_B$ vs $C_B[\eta]_I$.

To summarize, eqs 15 and 18 are valid for the cases $M_I/M_B > 3.52$ and $M_I/M_B < 1.43$, respectively. The data for τ for the PI-140/PB-63 system ($M_I/M_B = 2.22$) are expressed by neither eq 15 nor eq 18. In this case the motion of the PI chain is in the crossover region between the Zimm-like and reptation regimes, which are discussed in the following sections. The existence of the Zimm-like regime in condensed systems was reported by measurements of diffusion coefficients.[26,27]

2.4. General Representation of τ for Ternary Systems. In this section we attempt to express τ more generally including the case of $M_I \sim M_B$. In the previous section we indicated that τ is expressed by a universal function of $C_B[\eta]_B$ and $C_B[\eta]_I$. In the ternary system examined here, τ will be a function of N_I, N_B, and C_B. If the elementary process of the dynamics is the motion of the blobs, τ may be scaled by a form

$$\tau \simeq \tau_{blob} G'(N_I/g_B, N_B/g_B)$$
$$\simeq \tau_0 G(C_B[\eta]_I, C_B[\eta]_B) \qquad (20)$$

where G' and G represent functions. If this equation holds, the observed data points of τ for various M_I, M_B, and C_B should fall on a smooth universal surface in the three-dimensional space of τ vs $C_B[\eta]_I$ vs $C_B[\eta]_B$.

Figure 11 shows a contour diagram in which the iso-τ/τ_0 lines are plotted on the plane of $C_B[\eta]_I$ vs $C_B[\eta]_B$. The symbols plotted on the figure represent the interpolated values. We see that the contour line is smooth and monotonous over wide ranges of M_I, M_B, and C_B. This

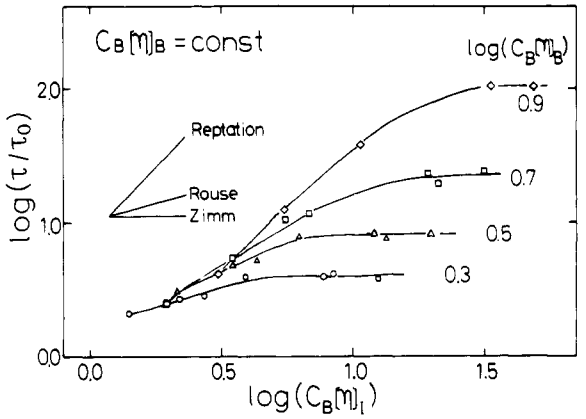

Figure 12. Double-logarithmic plot of τ/τ_0 against $C_B[\eta]_I$ at $C_B[\eta]_B$ = constant.

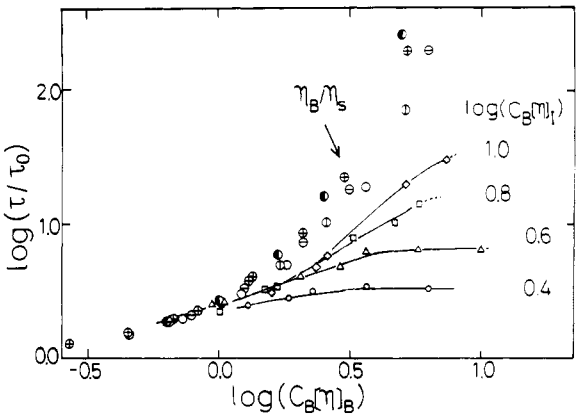

Figure 13. Double-logarithmic plot of τ/τ_0 against $C_B[\eta]_B$ at $C_B[\eta]_I$ = constant. For the sake of comparison, log η_B/η_s is also plotted.

fact indicates that eq 20 holds at least in the range examined here.

2.4.1. $C_B[\eta]_I$ Dependence of τ/τ_0. Figure 12 shows the cross-sectional view of Figure 11 at $C_B[\eta]_B$ = constant. Here we recall that the parameters $C_B[\eta]_I$ and $C_B[\eta]_B$ correspond to the number of blobs in the PI chain and the PB chain, respectively: $C_B[\eta]_I \simeq (N_I/g_B)^{3\nu-1}$ and $C_B[\eta]_B \simeq (N_B/g_B)^{3\nu-1}$. The number of blobs corresponds to the number of beads and the number of entanglements in the bead–spring model and the tube model, respectively. Thus, Figure 12 is equivalent to the M_I dependence of τ/τ_0 at fixed M_B. The N_I/g_B dependence of τ is generally expressed as

$$\tau \propto \tau_{blob}(N_I/g_B)^x \tag{21}$$

where $x = 3\nu$, 2.0, and 3, respectively, when the Zimm, Rouse, and tube theories are applicable. Here we neglected the numercial factor which is different for each case. Then the $C_B[\eta]_I$ dependence of τ/τ_0 is

$$\tau/\tau_0 \propto (C_B[\eta]_I)^{(x-3\nu)/(3\nu-1)} \tag{22}$$

where we used the relation $\tau_{blob} \propto \xi^3$ (eq 10). The exponent of this equation was calculated with $\nu = 0.56$, and the slopes of the $\log(\tau/\tau_0)$ vs $\log(C_B[\eta]_I)$ plot for $x = 3\nu$, 2, and 3 are indicated in Figure 12.

When $\log(C_B[\eta]_B) = 0.3$, the matrix PB chains are not entangled. In this case the slope in the range $\log(C_B[\eta]_I) < 0.7$ corresponds to the Rouse theory, but in the high $C_B[\eta]_I$ range the slope becomes zero, corresponding to the Zimm theory. Obviously the slope becomes zero at sufficiently low C_B. Thus, there exist two regimes in which τ conforms to the Zimm theory.

In the case of $\log(C_B[\eta]_B) = 0.9$, where the matrix chains are entangled, the slope in the range $0.5 < \log(C_B[\eta]_I) < 1.0$ is close to that for the reptation model. However, with increasing $C_B[\eta]_I$ the slope decreases and appears to flatten out. These facts indicate that if a guest chain is much longer than the matrix chain, the guest chain behaves like a Zimm chain whether the matrix is entangled or not.[26,27]

2.4.2. $C_B[\eta]_B$ Dependence of τ/τ_0. Figure 13 shows the cross-section view of Figure 11 at $\log(C_B[\eta]_I)$ = const, namely the M_B dependence of τ/τ_0 at fixed M_I. The data of matrix viscosity η_B/η_s are compared with τ/τ_0 data in this figure. With increasing $C_B[\eta]_B$ the matrix viscosity increases exponentially but τ/τ_0 becomes independent of $C_B[\eta]_B$ eventually. In this high $C_B[\eta]_B$ region the PB chains form a temporary network and the PI chain moves by a reptation mechanism irrelevant of the macroscopic matrix viscosity. But in low $C_B[\eta]_B$ the τ/τ_0 of PI is considered to reflect the matrix viscosity.

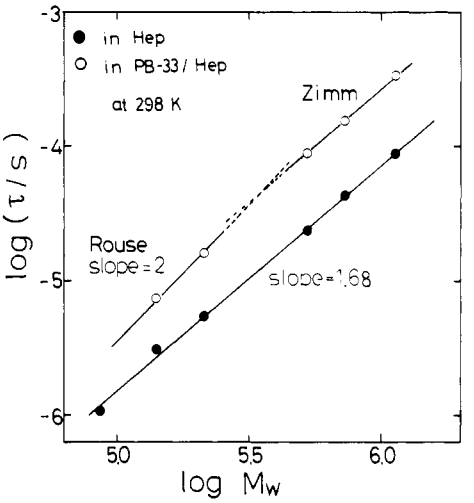

Figure 14. Double-logarithmic plot of τ vs M_I for binary solutions of PI/heptane (solid circle) and that for PI dissolved in PB-33/heptane solution (open circle).

2.5. M_I Dependence of τ. In this section we discuss the M_I dependence of τ at fixed C_B and M_B, specifically $C_B = 4.84 \times 10^{-2}$ g cm^{-3} and $M_B = 3.3 \times 10^4$. From the C_B dependence of η_B/η_s shown in Figure 7a, we see that PB chains are not entangled in these conditions. Figure 14 shows the comparison of the τ vs M_W curves of the PI molecules dissolved in *n*-heptane and that in PB/Hep semidilute solution. The plot for dilute heptane solutions conforms well to a straight line, and the slope is 1.68. This behavior can be explained by the Zimm theory in which the excluded-volume effect is taken into account ($\nu = 0.56$ in eq 2). The slope for the ternary systems in the high M_I region is the same as that for the binary systems. However, in the low M_I region, specifically for the data of $M_I = 1.40 \times 10^4$ and 2.13×10^4, the slope is equal to 2.0 and agrees with the Rouse theory (eq 3). This result strongly supports the conclusion given in the previous section; i.e., when M_I is much higher than M_B, the PI chain behaves like a Zimm chain, but when M_I is comparable to M_B, the hydrodynamic interaction is screened and the PI chain behaves like a Rouse chain.

Figure 15 shows the double-logarithmic plot of τ/τ_0 vs M_I. This figure corresponds well to Figure 12. The values of $(\eta_B/\eta_s)(r/r_0)^3$ are indicated in this figure to check eq 12. As seen in the figure, we also see that the matrix viscosity is higher than the relaxation time of PI exhibiting the Zimm-like behavior.

2.6. Classification of the Motion of PI Chain. Here we classify the dynamical states in the ternary system.

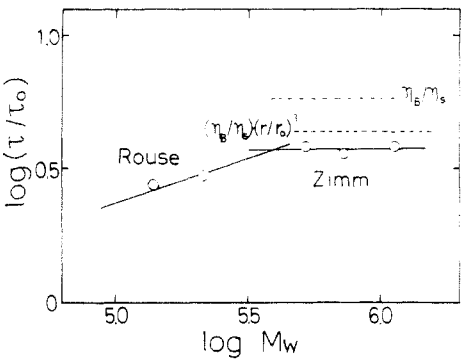

Figure 15. Double-logarithmic plot of τ/τ_0 for PI dissolved in PB-33/heptane solution. The values of η_B/η_s and (η_B/η_s) $(r/r_0)^3$ are indicated for comparison.

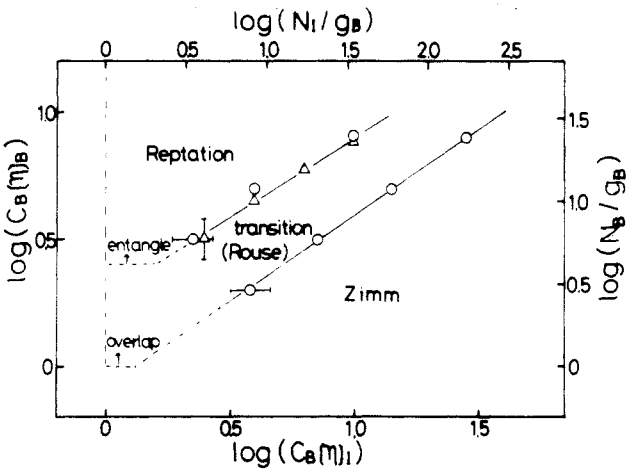

Figure 16. Dynamic state diagram indicating the crossover points between the regimes in which the dynamics of PI chains in the semidilute PB solutions is described by Zimm theory and tube theory. Intermediate region may be assigned to the Rouse regime.

The crossover points between the regimes in which τ conforms to the Zimm, Rouse, and the tube theories are determined by using Figures 12 and 13 and plotted on the log $C_B[\eta]_I$ vs log $C_B[\eta]_B$ plane (Figure 16). The concentration at which the PB chains begin to entangle each other (dashed line in Figure 16) is roughly estimated from the curves shown in Figure 7. The crossover is given by log $C_B[\eta]_B \simeq 0.4$; above this concentration the slope becomes $3.4/(3\nu - 1)$. In the case of $C_B[\eta]_I < 1$, the dimension of the PI chain is smaller than the screening length of PB solutions; thus, the PI chain may behave like a Zimm chain. When $C_B[\eta]_I \gg C_B[\eta]_B$, the PI chains move like a Zimm chain, but in the opposite case of $C_B[\eta]_I \ll C_B[\eta]_B$, they move by the reptation mechanism.

2.7. Shape of ϵ'' Curves. In section 1.2 we demonstrated that the shape of ϵ'' curves for PI/Hep binary solutions changes with PI concentration (see Figure 4). For ternary solutions the C_B dependence of ϵ'' curves is shown in Figure 17. We see that the shape in PI-743/PB-521 changes with C_B but does not in PI-743/PB-211 in a similar C_B range. We see that this behavior corresponds well to that of the binary PI/heptane systems.

For the binary PI/heptane systems, we observed that the width increased in the crossover region beween the dilute and semidilute regimes but the width becomes independent of concentration when the topological interaction becomes predominant. According to the classification of the dynamics of the PI chains (Figure 16), the PI-743/PB-211 and PI-743/PB-521 systems locate in the Zimm to Rouse regime and the Rouse to reptation regime,

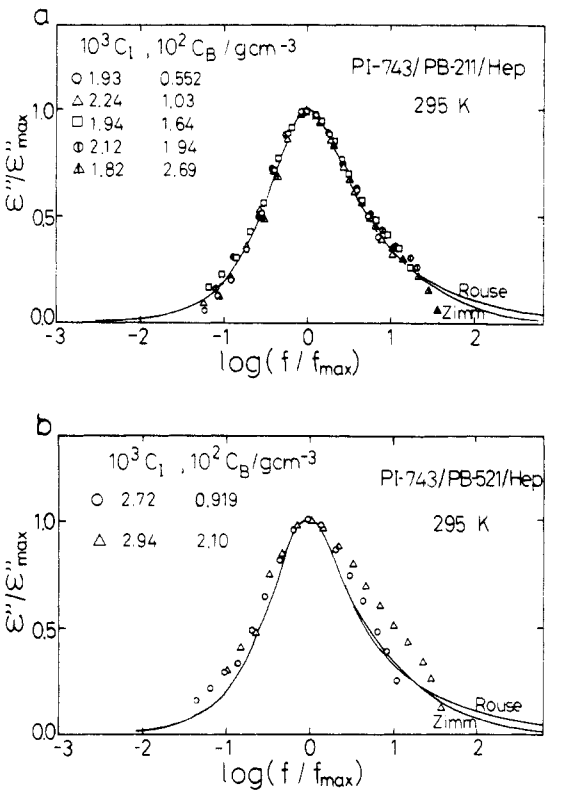

Figure 17. Normalized ϵ'' curves for (a) PI-743/PB-211/heptane and (b) PI-743/PB-521/heptane.

respectively. Thus, we see that the phenomenon observed in Figure 17 is quite consistent with that in the binary systems.

Conclusion

1. In the binary PI/heptane solutions, the dielectric normal mode relaxation time τ of PI conforms well to the Muthukumar–Freed theory. The parameter A of eq 9 is equal to $0.29[\eta]$.

2. In the binary PI/heptane solutions, the width of the ϵ'' curve begins to increase around $C_I = C_I^*$, but when the PI chains are fully entangled, the width becomes independent of C_I.

3. We found that τ of PI in ternary PI/PB/heptane solutions was expressed by the following scaling form:

$$\tau/\tau_0 \simeq G(C_B[\eta]_I, C_B[\eta]_B)$$

4. In the ternary solutions, the $\log(\tau/\tau_0)$ vs $\log(C_B[\eta]_I)$ curves exhibit sigmoidal shape. This indicates that the dynamics of the guest PI chain in PB solutions changes from Zimm-like behavior at infinite dilution to Rouse-like and reptation mechanisms with increasing $C_B[\eta]_I$. With further increase of $C_B[\eta]_I$, it changes again to Zimm-like.

5. The width of the ϵ'' curve of the ternary system changes in the Rouse regime but does not change in the Zimm and reptation regimes.

Acknowledgment. This work was partly supported by the Institute of Polymer Research, Osaka University.

References and Notes

(1) Urakawa, O.; Adachi, K.; Kotaka, T. *Macromolecules*, previous paper in this issue.
(2) Ferry, J. D. *Viscoelastic Properties of Polymers*, 3rd ed.; Wiley: New York, 1980.
(3) Doi, M.; Edwards, S. F. *The Theory of Polymer Dynamics*; Clarendon: Oxford, U.K., 1986.
(4) Stockmayer, W. H. *Pure Appl. Chem.* **1967**, *15*, 539.

(5) Stockmayer, W. H.; Bauer, M. E. *J. Am. Chem. Soc.* **1964**, *86*, 3485.
(6) Adachi, K.; Kotaka, T. *Macromolecules* **1988**, *21*, 157.
(7) Adachi, K.; Okazaki, H.; Kotaka, T. *Macromolecules* **1985**, *18*, 1687.
(8) Adachi, K.; Imanishi, Y.; Shinkado, T.; Kotaka, T. *Macromolecules* **1989**, *22*, 2391.
(9) Baysal, B. M.; Stockmayer, W. H. *J. Mol. Liq.* **1993**, in press.
(10) Wheeler, L. M.; Lodge, T. P.; Hanley, B.; Tirrell, M. *Macromolecules* **1987**, *20*, 1120.
(11) Nemoto, N.; Okada, S.; Kurata, M. *Macromolecules* **1988**, *21*, 1502.
(12) Numasawa, N.; Kuwamoto, K.; Nose, T. *Macromolecules* **1986**, *19*, 2593.
(13) Rouse, P. E. *J. Chem. Phys.* **1953**, *21*, 1272.
(14) Zimm, B. H. *J. Chem. Phys.* **1956**, *24*, 269.
(15) de Gennes, P.-G. *J. Chem. Phys.* **1971**, *55*, 572.
(16) Doi, M.; Edwards. S. F. *J. Chem. Soc., Faraday Trans. 2* **1978**, 74, 1789, 1802, 1818.
(17) de Gennes, P.-G. *Scaling Concept in Polymer Physics*; Cornell University Press: Ithaca, NY, 1979.
(18) de Gennes, P.-G. *Macromolecules* 1976, *9*, 587, 594.
(19) Takahashi, Y.; Isono, Y.; Noda, I.; Nagasawa. *Macromolecules* **1985**, *18*, 1002.
(20) Muthukumar, M.; Freed, K. F. *Macromolecules* **1978**, *11*, 843.
(21) Muthukumar, M. *Macromolecules* **1984**, *17*, 971.
(22) Patel, S. S.; Takahashi, K. M. *Macromolecules* **1992**, *25*, 4382.
(23) Adam, M.; Delsanti, M. *J. Phys. (Paris)* **1984**, *45*, 1513.
(24) Osaki, K.; Nishimura, Y.; Kurata, M. *Macromolecules* **1985**, *18*, 1153.
(25) Colby, R. H.; Rubinstein, M. *Macromolecules* **1990**, *23*, 2753.
(26) Antonietti, M.; Coutandin, J.; Sillescu, H. *Macromolecules* **1986**, *19*, 793.
(27) Green, P. F.; Kramer, E. J. *Macromolecules* **1986**, *19*, 1108.